Cluster structure of ^{11}C investigated with a breakup reaction

Ziming Li,[1] Jie Zhu,[2] Taofeng Wang,[2,*] Minliang Liu,[3] Jiansong Wang,[3] Yanyun Yang,[3] Chengjian Lin,[4] Junbing Ma,[3] Peng Ma,[3] Zhen Bai,[3] Yuechao Yu,[3] Xing Zhang,[3] Xingquan Liu,[3] Fangfang Duan,[3] Chengui Lu,[3] Herun Yang,[3] Xianglun Wei,[3] Junwei Zhang,[3] Shilun Jin,[3] Zhihao Gao,[3] Yue Hu,[2] Yongjin Yao,[2] Jianguo Wang,[3] Song Guo,[3] Wei Jiang,[5] Biao Yang,[5] and Jianjun He[1,6,†]

[1]*Key Laboratory of Beam Technology of Ministry of Education, College of Nuclear Science and Technology, Beijing Normal University, Beijing 100875, China*

[2]*School of Physics, Beihang University, Beijing 100191, China*

[3]*Institute of Modern Physics, Chinese Academy of Sciences, Lanzhou 730000, China*

[4]*China Institute of Atomic Energy, P.O. Box 275 (10), Beijing 102413, China*

[5]*State Key Laboratory of Nuclear Physics and Technology, School of Physics, Peking University, Beijing 100871, China*

[6]*Institute of Radiation Technology, Beijing Academy of Science and Technology, Beijing 100875, China*

(Received 3 May 2022; revised 16 September 2022; accepted 11 January 2023; published 25 January 2023)

The excitation spectra above the breakup threshold of ^{11}C were measured using the invariant mass method with a 25.0-MeV/nucleon beam bombarding a carbon target for the first time. This measurement was performed with a zero-degree double-sided silicon strip detector together with four CsI(Tl) detectors, which could detect breakup fragments with low relative kinetic energy. Some resonances in ^{11}C were clearly observed in the excitation energy range of 8–14 MeV proceeding through the ^{7}Be + α channel. Among them, a resonance with the largest yield was observed around 8.10 MeV. We assign it as the head of the $K^{\pi} = 3/2^{-}$ rotational band, and suggest the 9.38-MeV state as the second member of this band.

DOI: 10.1103/PhysRevC.107.014320

I. INTRODUCTION

Clustering is an important phenomenon that appears in many kinds of systems. In atomic nuclei, nucleons can be grouped into clusters for stability [1,2]. This gives rise to some resonances with clustered rather than compacted configuration, especially the resonances just above the threshold of cluster decay, which were predicted by Ikeda *et al.* in 1968 [3]. From an experimental perspective, the energy and spin parity of excited states have been analyzed to build rotational bands with large inertia momentum, which indicates very large deformation according to the cluster interpretation. In past decades, charged-particle spectroscopy has been greatly developed and the measurement of the typical decay of cluster states has attracted much attention [4]. The predominating decay channel can provide essential evidence for the cluster states.

The alpha cluster plays an important role in light nuclei. In an early study, an alpha-particle model was proposed to describe the α-conjugated nuclei [5]. The ground state of ^{8}Be displays a dumbbell shape with two α particles separated [6]. Similarly, the Hoyle state of ^{12}C is regarded as an α condensate [7] with its structure still unsettled [8], first known due to its astrophysical importance [9].

In recent years, the molecular orbital structure has been studied extensively, in which the additional neutron acts as a valence neutron, similar to the valence electron in molecules, helping to stabilize the nucleus [1]. However, there have been few studies about cluster states in neutron-deficient nuclei. ^{11}C has one neutron less than ^{12}C, with a structure similar to its mirror nucleus ^{11}B [10]. Based on calculations of the antisymmetrized molecular dynamics (AMD) [11,12], the generator coordinate method [12], and the orthogonality condition model [13], the $3/2^{-}_{3}$ states in ^{11}C (^{11}B) were suggested to be $2\alpha + {}^{3}\mathrm{He}(t)$ cluster states, which are analogous to the Hoyle state. In experimental studies, the Gamow-Teller (GT) transition from ^{11}B to ^{11}C ($3/2^{-}_{3}$) was measured to be abnormally weak [14], indicating that the $3/2^{-}_{3}$ state is very different from the ground state in ^{11}B (^{11}C) and might possess a cluster structure. The enhanced monopole transition strength in ^{11}B ($3/2^{-}_{3}$, 8.56 MeV) [15] agrees well with the AMD prediction [11], providing important evidence of cluster structure. Thus, a similar structure was expected for ^{11}C. Many resonances were observed in the study of the ^{16}O(^{9}Be, α^{7}Be)^{14}C reaction, from which two even-parity rotational bands with large inertia momentum were established [16,17]. However, only a small amount of yield was observed at approximately 8.10 MeV in the excitation function, raising doubts as to whether the $3/2^{-}_{3}$ state is a cluster state. Later, resonant (α, α) scattering and (α, p) reaction were measured by two research groups and independently deduced resonance information in ^{11}C [18,19], and a new $K^{\pi} = 3/2^{-}$ rotational band was proposed, but the head of this band was not

*tfwang@buaa.edu.cn
†hejianjun@bnu.edu.cn

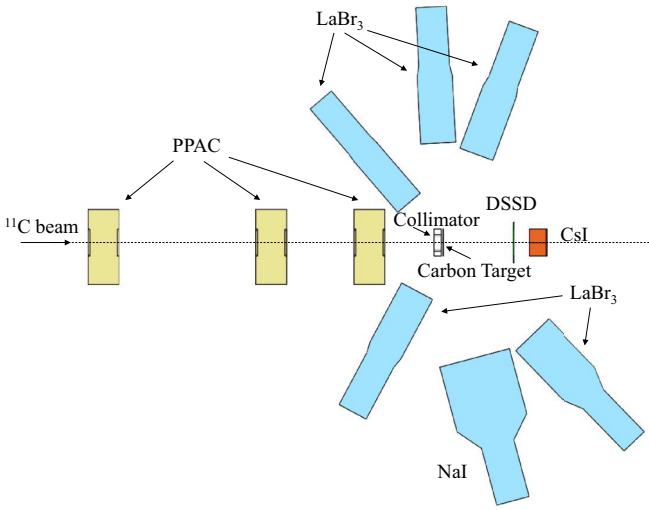

FIG. 1. Schematic view of the experimental setup at the T2 position of RIBLL1.

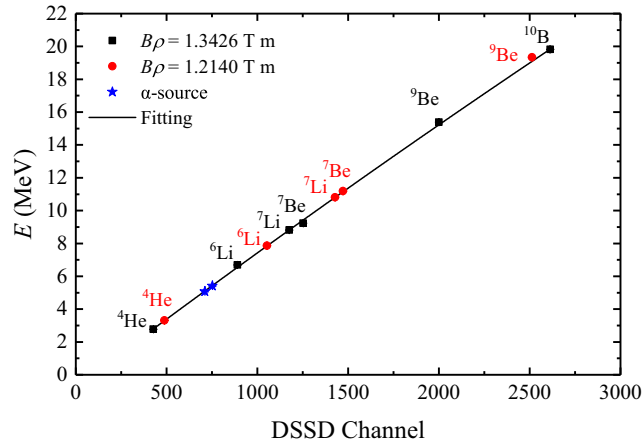

FIG. 2. The energy calibration of DSSD by beam impurities.

covered, due to its energy being close to the α-decay threshold ($E_{\rm rel} = 0.56$ MeV). The $3/2_3^-$ state in ^{11}C was very likely to possess a three-center cluster structure, but further experimental evidence is needed to draw a decisive conclusion.

In the present paper, we performed measurements of the ^{12}C(^{11}C, α^7Be) reaction to study the resonance states in ^{11}C, especially the $3/2_3^-$ state at approximately 8.10 MeV, with the aim of finding evidence of cluster structure. A zero-degree telescope was exploited to increase the detection efficiency near the threshold. The invariant-mass method was applied to analyze the α-decay channel, and the relevant rotational bands were discussed.

II. EXPERIMENT

The experiment was performed at the radioactive ion beam line at the heavy ion research facility in Lanzhou (HIRFL-RIBLL1) [20,21]. A primary beam of 60-MeV/nucleon $^{12}C^{6+}$ bombarded a 3.5-mm beryllium target with an intensity up to 30 enA. With RIBLL1, a secondary beam of ^{11}C particles was selected and optimized, with an intensity of approximately 1×10^4 pps and a purity over 99%. The beam particles were identified by the $B\rho - \text{TOF} - \Delta E$ method [22]. Here, TOF represents the time of flight between the first plastic scintillator (start at the T1 focal plane) and the second one (stop at the T2 focal plane), where the flight path is 16.69 m [23]. The experimental setup in the RIBLL1 T2 focal plane is schematically shown in Fig. 1. Three parallel plate avalanche chambers (PPACs) were placed along the beam direction to track the beam. PPACs have a delay-line readout, with a position resolution of 1 mm and efficiency of each plate varying from 30 to 70%. The self-supporting carbon target with a thickness of 50 mg/cm^2 ($\phi = 30$ mm) was utilized as the secondary target. After passing through three PPACs, the energy of the ^{11}C beam is deduced to be 25.0 MeV/nucleon at the midtarget position with a SRIM code [24].

A set of ΔE-E telescopes was placed in the downstream zero-degree direction to pick up the fragments, consisting of a W1-type double-sided silicon strip detector (DSSD) [25] and a 2×2 CsI(Tl) scintillator array, with an angular coverage of 0°–9°. The DSSD is 148 μm thick, with an active area of 50×50 mm^2, and 16×16 strips. Each CsI(Tl) scintillator unit ($25 \times 25 \times 30$ mm^3 in size) has a 10-μm-thick window, and a photodiode readout at its back. Five $LaBr_3$(Ce) scintillators and one NaI(Tl) scintillator were mounted around the target to detect the deexcited γ rays from ^{7}Be*($1/2^-$, 429 keV), covering approximately 10% of the 4π solid angle.

In this kind of work, the energy calibration of DSSD is very important, because it determines the total kinetic energies of the fragments deposited in the DSSD, and subsequently determines the reconstructed excitation energy of ^{11}C. At first, we made the beam energy calibration by the beam impurities. Different beam impurities have almost the same $B\rho$ and the length of flight, thus their times of flight are proportional to their m/q. After performing linear regression on the time of flight, the $B\rho$ as well as the kinetic energy of each nucleus can be computed from the slope. To take special relativity into account, each m/q and kinetic energy are recalculated after linear regression. This procedure is repeated several times, until the $B\rho$ and the kinetic energies have converged. The resulting $B\rho$ value turned out to be 3.3% larger than that nominal magnet-setting $B\rho$ value during the experiment. This correction factor is helpful for future RIBLL1 magnet settings. The accuracy of TOF played an important role in the DSSD calibration. Here, the full width at half maximum (FWHM) of TOF is 3 ns for ^{11}C and ≈2 ns for the impurities, and hence the uncertainty of ^{11}C beam energy is determined to be ≈2.4% in the midtarget position.

Figure 2 shows the DSSD energy calibration for major beam impurities, where the deposited energies in the DSSD were calculated by a LISE++ code [26], ranging from 2.8 to 20 MeV, providing six calibration points for each group of runs. The same procedure was also applied to the data with different $B\rho$ values, and all the results were consistent. The calibration performed with a standard α source of ^{239}Pu and ^{241}Am was in good agreement with the former method (see Fig. 2). The dead-layer thickness of the DSSD was determined to be 0.5 μm. An energy resolution of 52 keV (FWHM) was achieved for the 5.157-MeV α particles.

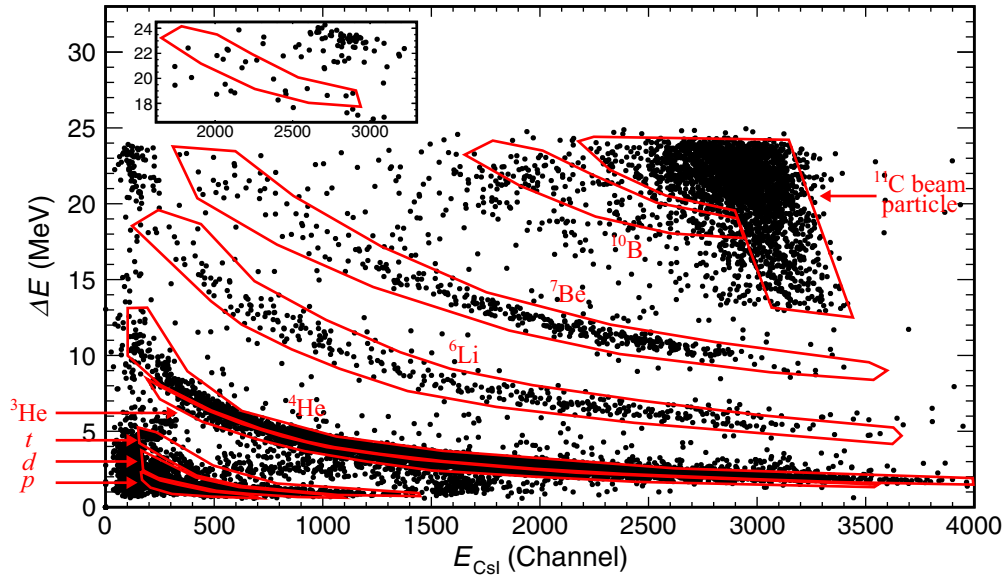

FIG. 3. The ΔE–E spectrum for particle identification. The inserted figure shows the ^{10}B particles detected by those pixels shielded by a 30-mm collimator (i.e., gated by the region outside of the beam spot).

Four CsI(Tl) scintillators were used together with the DSSD to identify the fragments. Because of the particle-dependent response of CsI(Tl) [27], its absolute energy calibration was not performed in this paper owing to the limited machine time. Therefore, we have to calculate the total energies of fragments by using the SRIM code, based on the energies deposited on the DSSD. And that is why the presently deduced resonance energies slightly deviate from the literature values, as shown in Sec. IV. The $LaBr_3$(Ce) and NaI(Tl) scintillators were calibrated with the standard ^{152}Eu γ-ray source and the intrinsic radiation from ^{138}La [28].

III. RESULTS

In the present paper, beam particles were tracked by three PPACs, from which the hit positions were derived. The fragments were detected and identified by different segments of the telescope separately, giving energy and emission angle information. Figure 3 shows the ΔE–E particle identification spectrum. The proton (p), deuteron (d), and triton (t) particles are separated clearly, and ^{7}Be can be picked out unambiguously. However, the loci of ^{3}He and ^{4}He are relatively close, and thus those events near the boundary must be rejected. A portion of the ^{10}B locus is heavily contaminated by the intense ^{11}C beam particles, while it can be identified in those pixels shielded by a ϕ30-mm collimator (see Fig. 1) placed in front of the target (see the inset in Fig. 3).

In the present analysis procedure, the number of particles detected by the DSSD is obtained by correlating the front and back sides of the DSSD signals. Here, "twofold" first means two particles are detected by the DSSD. The corresponding signals of CsI, the coordinates of which are calculated by extrapolating the position information of DSSD, are then taken out and plotted in Fig. 3. Only the particles that can be identified could have the opportunity to enter the subsequent calculations, including Q value, excitation energy, etc. Thus, "twofold" secondly means two particles are identified by the DSSD-CsI, when specific particles are concerned. In this way, the coincidence events were selected, and the relative energy ($E_{\rm rel}$) between two fragments was reconstructed from their masses (m_a, m_b), their kinetic energies (T_a, T_b), and the angle (θ) between their momenta. According to the invariant-mass method, the excitation energy (E_x) of ^{11}C equals relative energy ($E_{\rm rel}$) plus threshold energy ($E_{\rm thr}$) of the corresponding cluster decay [29]:

$$\begin{aligned} E_x &= (M - M_0)c^2 = E_{\rm rel} + E_{\rm thr} \\ \text{with } M^2c^4 &= (E_a + E_b)^2 - |P_a + P_b|^2c^2 \\ &= m_a^2c^4 + m_b^2c^4 + 2(m_ac^2 + T_a)(m_bc^2 + T_b) \\ &\quad - 2\sqrt{\left(T_a^2 + 2m_aT_a\right)\left(T_b^2 + 2m_bT_b\right)}\cos\theta. \end{aligned}$$

The validity for the energy determination of the fragments as well as the invariant-mass method has been checked by the $^6\text{Li} \to \alpha + d$, $^7\text{Be} \to \alpha + {}^3\text{He}$, $^8\text{Be} \to 2\alpha$, and $^{10}\text{B} \to {}^6\text{Li} + \alpha$ channels, as shown in Fig. 4. Regarding fragments, ^{4}He or α can always be treated at its ground state in the present energy regime. However, the contribution from the excited states in ^{7}Be and ^{10}B cannot be ignored simply.

In the earlier studies, both the total energy spectrum [16] and the Q-value spectrum [30] were analyzed to discriminate different reaction channels. The excited states in fragments could be identified if the resolution is good enough. Here, Q value is reconstructed as the difference between the total exit ($T_{\rm tot}$) and entrance ($T_{\rm beam}$) kinetic energies:

$$\begin{aligned} Q &= T_{\rm tot} - T_{\rm beam}, \\ T_{\rm tot} &= T_a + T_b + T_r \end{aligned}$$

where $T_{\rm beam}$ and T_r are the kinetic energies of the beam particle ^{11}C and the recoil particle ^{12}C, respectively. In practice, the total energy spectrum and the Q-value spectrum are equivalent

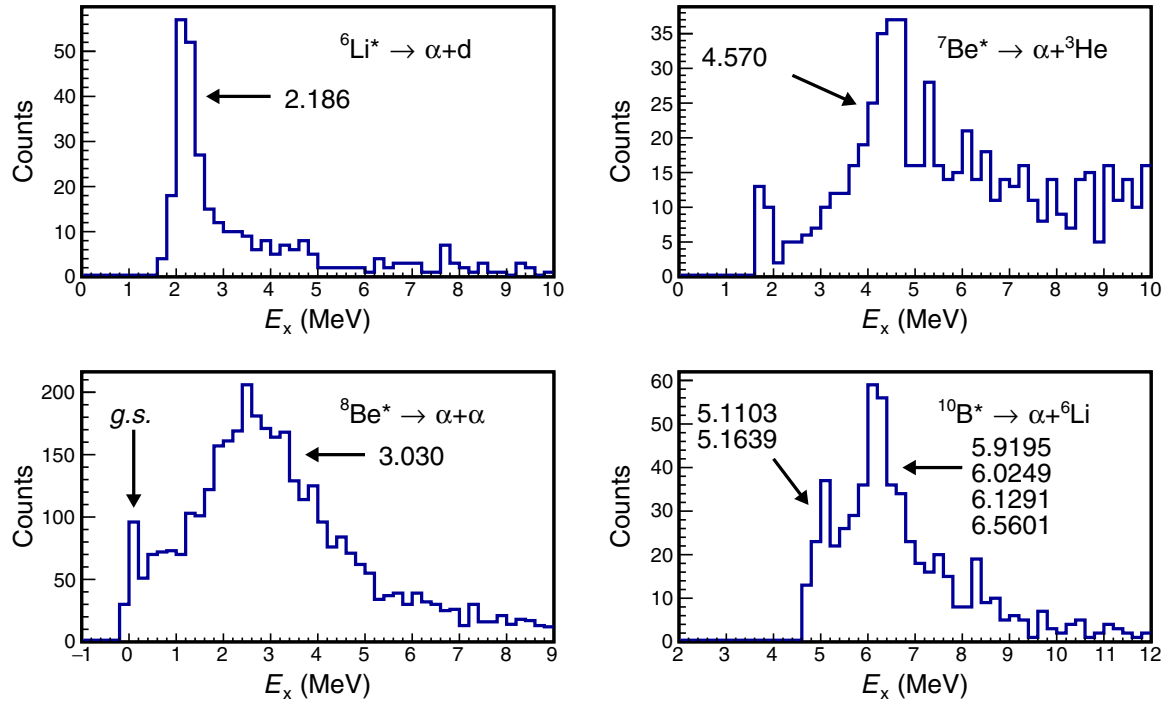

FIG. 4. The invariant-mass spectra reconstructed for different product combinations. Here, the energies labeled at the peaks are adopted from ENSDF [31].

in our paper, and thus we analyzed only the Q-value spectrum. For the ^{12}C recoils not detected in coincidence, their kinematic energies (T_r) had to be estimated from the conservation of momentum, with uncertainties from beam energy:

$$T_r = \sqrt{m_r^2c^4 + P_r^2c^2} - m_rc^2$$
$$= \sqrt{m_r^2c^4 + |P_{\text{beam}} - P_a - P_b|^2c^2} - m_rc^2$$

where P_{beam} and P_r are the momenta of the beam particle ^{11}C and the recoil particle ^{12}C, respectively. Here, m_r is taken as the rest mass of the ^{12}C in its ground state. Assuming that the reaction takes place at the middle of the target, the energy loss in the target has been considered for each particle. The uncertainties mentioned above, together with the accidental coincidence and other reaction channels such as ^{12}C excitation, lead to the poor resolution of the Q-value spectrum (as shown in Fig. 5). In fact, it is impossible to identify the very low 429-keV $1/2^-$ state in ^{7}Be for this technique. We employed six scintillation detectors to evaluate the contribution of this 429-keV γ ray emitted by the exited ^{7}Be, and its low statistics possibly implies a relatively small branching ratio of α_1 (α decay to the excited state in ^{7}Be) for most resonances, which is consistent with the previous conclusions [16,19]. Nonetheless, the Q-value spectrum with certain restricted conditions may help to suppress the contribution from other reaction channels and the accidental coincidence events as discussed in the subsection.

The excitation energy spectra of ^{11}C were reconstructed from α_0-decay ($^{11}\text{C}^* \rightarrow \alpha + {}^{7}\text{Be}$, $Q = -7.545$ MeV [31]) and p_0-decay ($^{11}\text{C}^* \rightarrow p + {}^{10}\text{B}$, $Q = -8.69$ MeV [31])

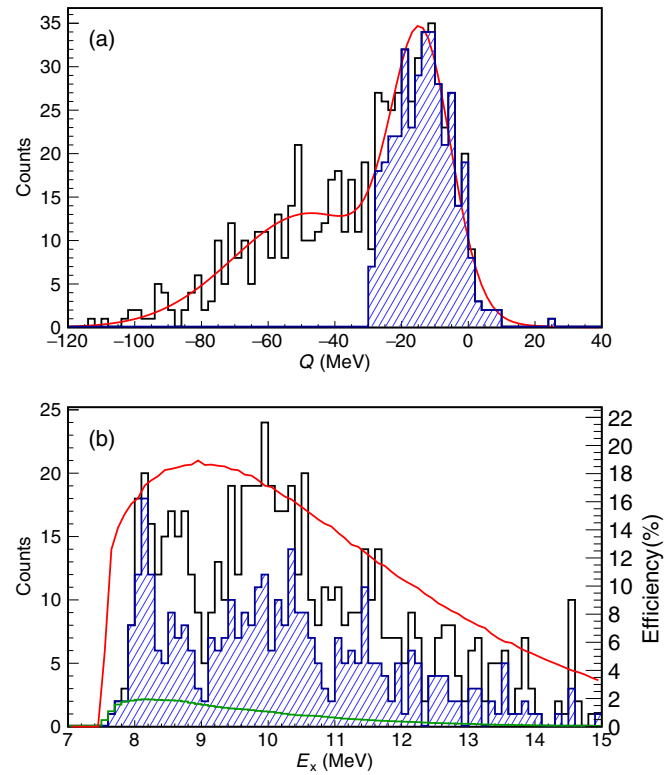

FIG. 5. For the $^{11}\text{C}^* \rightarrow \alpha + {}^{7}\text{Be}$ case: (a) Raw Q-value spectra (black) with fitting curve (red) and cut spectrum (blue shaded); (b) raw E_x spectrum (black) and cut E_x spectrum (blue-shaded). The cut "event-mixing" spectrum (green) and efficiency curve (red) are also shown.

channels, respectively. Here, α_0 and p_0 represent the decay to the ground states in ^{7}Be and ^{10}B, respectively. Only seven valid events were observed in proton decay at E_x near 10.0 and 11.1 MeV, since the proton events were heavily polluted by the electronics noise of DSSD (as seen in Fig. 3), and we set a relatively high noise threshold for DSSD, in which the energy deposition of the most energetic protons was less than 1 MeV. A lot of proton events were lost in the acquisition, and hence it is difficult to analyze the proton-decay channel. In this paper, we only focus on the α-decay channel.

A. ^{11}C* → $\alpha + ^7$Be

It should be noted that α_0 decay is known to be the predominant channel for most resonances from 8.9 to 13 MeV in ^{11}C [18,19], which is also the primary interest of the present paper. In Fig. 5(a), the raw Q-value spectrum (black curve) has two components: a wide Gaussian component with a center at approximately −40 MeV might be the background from other reaction channels or the accidental coincidence events, and the $Q > -30$ MeV part standing out from the background corresponds to the real coincidence events (filled area). The fitting with the sum of two Gaussian functions shows that the background part contributes about 27% in the $Q > -30$ MeV region. Without the detection of the recoil target nucleus, there would be many sources in the background. The breakup of recoil ^{12}C would contribute to the background, when one of the 3α particles emitted by ^{12}C was detected, which tends to have lower kinematic energy. The particles scattered by the detector and target supporting structures may also be detected. The raw excitation function (black curve) is drawn in Fig. 5(b), in which a strong peak near 8.10 MeV is observed. It still requires further background subtraction and energy-dependent efficiency correction, as discussed below.

A Monte Carlo simulation was performed to give the energy-dependent efficiency of coincidence detection, as well as the reasonable energy range of detected α. The energy loss in materials was calculated by the SRIM code since its output can be conveniently utilized in the simulation. The angular distribution of inelastic scattering of the ^{11}C beam on the ^{12}C target was sampled in a Gaussian distribution for simplicity, and the α decay of ^{11}C was assumed to be isotropic [30,32] in the center-of-mass frame. The uncertainties of energy and angle of beam, reaction position and depth, energy and angular staggering in the material, as well as detector resolution were included in the simulation. The coincidence events were counted with respect to an excitation energy of ^{11}C, excluding those in which two fragments hit the same CsI(Tl) crystal or the same pixel of DSSD. The Monte Carlo simulated efficiency curve is drawn in Fig. 5(b), and a typical efficiency at 8.10 MeV is approximately 17%.

To suppress the background from the low-energy particles, upper limits of ΔE could be set as 3.8 MeV for alpha and 13.3 MeV for ^{7}Be, according to the simulated ΔE distribution of fragments. After applying this cut to the Q-value spectrum, the $Q < -30$ MeV part was reduced significantly, while the $Q > -30$ MeV part was reduced slightly. Thus, we took the $Q < -30$ MeV part as the background, and applied the Q-value cut and the ΔE cut to the raw spectrum to obtain a cleaner spectrum. It should be noted that the main reason for making this Q-value cut is to remove the contaminants from other reaction channels or accidental coincidence events. In this paper, the uncertainty in the reconstructed excitation energy was estimated to be ≈0.12 MeV, mainly contributed by those of the target position and energy calibration. The resolution of the reconstructed excitation energy was simulated to be ≈0.4 MeV (FWHM).

Figure 6 shows the efficiency-corrected excitation function for the $\alpha + ^7$Be channel, where the background from the direct breakup estimated by the "event-mixing" technique [29,33] was subtracted accordingly. In practice, one ^{7}Be nucleus is picked up from an experimental event, and one α particle from another event, then the invariant mass of the simulated ^{11}C nucleus is computed. The acceptance of the detectors and other experimental effects are contained simultaneously in the distribution obtained by this technique.

Because the decay width of most resonances is not as large as the resolution of the excitation function, the Gaussian fitting was performed to the expected resonances [8,18,19,31,34,35], by using the maximum likelihood method. Except for the statistical error, the systematic error was estimated to be ≈10%, mainly consisting of the uncertainties from the background and efficiency. Here, the uncertainty of the ^{12}C target thickness (50 mg/cm^2) is less than 5%, which was neglected in this paper. The cross section of the reaction through the 8.10-MeV resonance was determined to be 22.7 ± 7.0 mb.

It should be noted that the present experimental spectra have been analyzed as all transitions to the ground state. And the possible small α_1 contribution can be covered by the very large uncertainties as shown in Fig. 6. Here, we still would like to use the α symbol rather than α_0 or α_1; after all we cannot distinguish these two channels.

B. ^{11}C* → 2$\alpha + ^3$He

As the structure of ^{11}C was described as a three-center cluster, triplefold coincidence of $2\alpha + ^3$He was also analyzed (^{11}C* → $2\alpha + ^3$He, $Q = -9.132$ MeV). Such a reaction mechanism can often be analyzed via a Dalitz plot, but the statistics in this paper is too low to draw a readable plot. Its efficiency is approximately a quarter of that of the $\alpha + ^7$Be channel. The $E_{\rm rel}$ energies for the α-α pair and α-^{3}He pair have been reconstructed as shown in Fig. 7, respectively. The ground state and the 3.03-MeV state in ^{8}Be and the 4.57-, 6.73-, 7.21-, 9.27-, and 11.01-MeV states in ^{7}Be were very weakly observed as indicated in the figure, respectively. These excitation energies (indicated in the brackets) are adopted from ENSDF [31], by which the relative energies are calculated as also shown in Fig. 7. This result is similar to that of ^{11}B studied by Soić *et al.* [17], which possibly implies some three-center cluster structures existing in ^{11}C. However, due to the present low statistics, no further analysis was performed.

If ^{7}Be produced by ^{11}C α decay is in a higher excited state (over an α threshold of 1.587 MeV), then ^{7}Be will further decay, and thus three particles might be detected. Since there are few three-particle events observed in this experiment, the

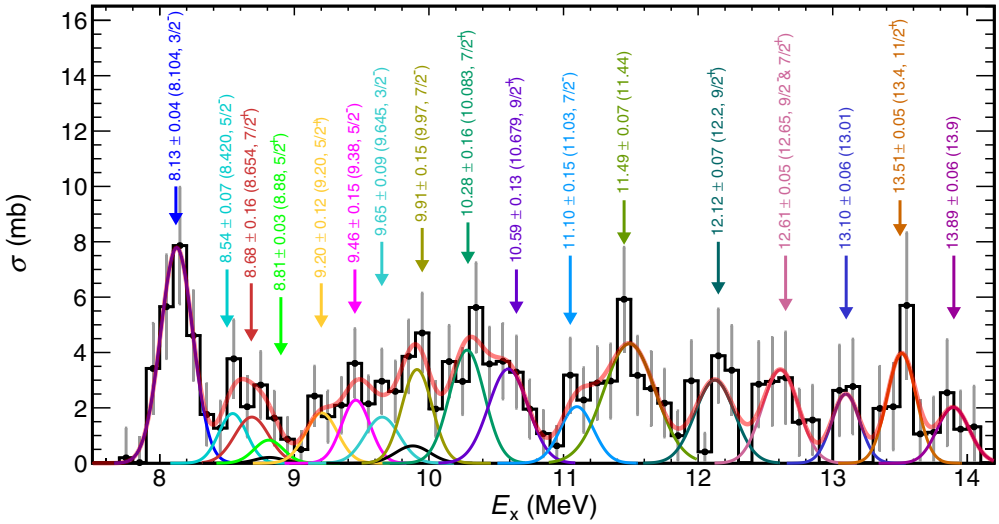

FIG. 6. Gaussian fitting to the excitation function (bin width = 0.1 MeV). Some states with amplitude $A > 0.8$ are indicated by arrows, and the total fit is shown by the red bold line. The numbers outside the parentheses are the present fitting results, and those inside are adopted from Refs. [16,19,31,34].

branch ratio of ^{7}Be in the higher excited state should be very small. Therefore, the cross section of ^{11}C α decay to the ground state in ^{7}Be is regarded as the total one in this paper.

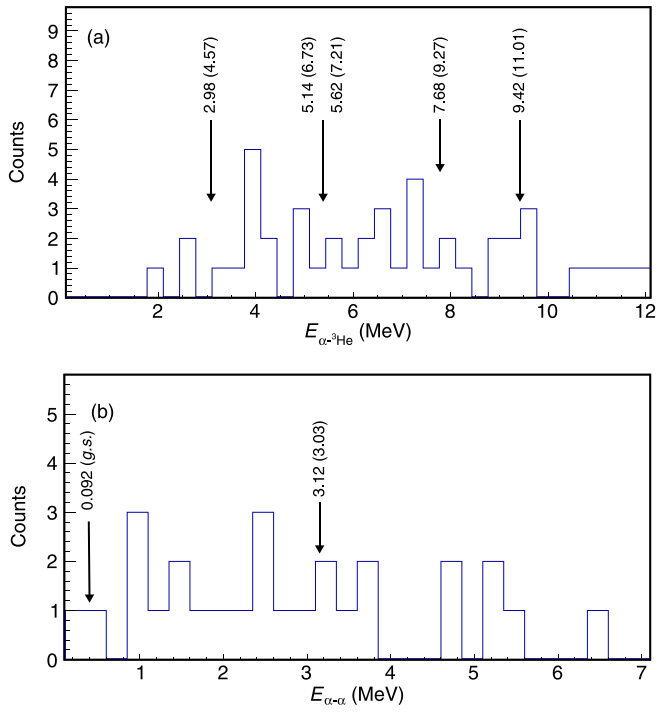

FIG. 7. (a) Reconstructed E_{rel} spectrum for the α-^{3}He pair (might decay through ^{7}Be). (b) Reconstructed E_{rel} spectrum for the α-α pair (might decay through ^{8}Be). Here, the relative energies are calculated from the corresponding excitation energies (listed in the parentheses from ENSDF [31]).

IV. DISCUSSION

A. Resonance states

The 8.10-MeV state has been studied via many reactions, giving $\Gamma \approx 6$ eV and $\Gamma_\alpha/\Gamma \approx 94.5\%$ [31]. Moreover, its abnormally small proton spectroscopic factor [10] and the GT transition strength [14] also indicated a cluster structure. In Fig. 6, the strongest peak at approximately 8.10 MeV indicates a strong transition from the ground state ($3/2^-_1$) to the 8.10-MeV state ($3/2^-_3$), which is quite different from the excitation function reconstructed in the ^{16}O(^{9}Be, α^{7}Be)^{14}C reaction [16]. The detectors in both experiments were placed in forward angles, so this difference may be mainly due to a different reaction mechanism and energy. The $2p$ pickup reaction might be more likely to populate two-particle excited states in some energy regions, while inelastic excitation can populate a cluster state via monopole transition ($3/2^- \rightarrow 3/2^-$). This would be important evidence that the $3/2^-_3$ state is a cluster state.

Around 8.90 and 9.35 MeV, there are expected to be two resonances. In the previous measurement of reaction ^{10}B(p, α)^{7}Be, Lombardo *et al.* [35] proposed a new resonance at 9.36 MeV ($5/2^-$), and later Wiescher *et al.* [34] claimed that there should be two resonances at 8.88 ($5/2^+$) and 9.38 MeV ($5/2^-$). The 9.38-MeV state was observed in our paper, while the 8.88-MeV state was not sufficiently obvious, being overlapped with the doublet near 8.7 MeV.

In the resonant scattering of ^{7}Be+α studied by Yamaguchi *et al.* [19], two strong resonances were observed at 12.40 and 12.65 MeV in the 12.0 − 13.0-meV region. Here, we observed them at 12.1 and 12.6 MeV, respectively, which agree with the previous results within the uncertainties. In addition, in the mirror ^{11}B nucleus, there is a doublet consisting of the 13.14-MeV state ($9/2^-$) and the 13.16-MeV state ($7/2^+$), and hence ^{11}C might have a similar doublet structure near 12.65 MeV. The $7/2^+$ state observed in the ^{10}B(p, α)^{7}Be reaction

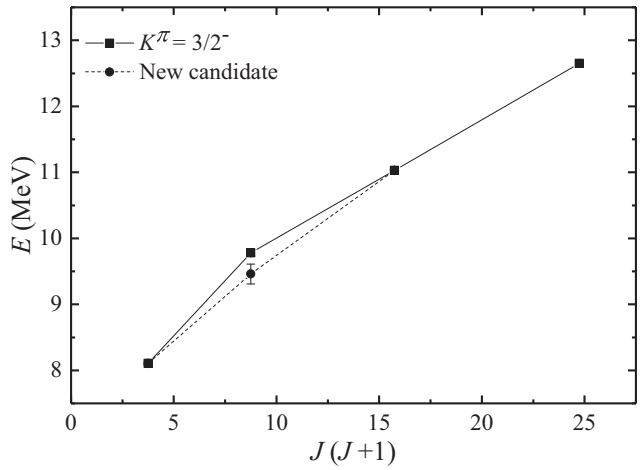

FIG. 8. The negative-parity rotational band ($K^\pi = 3/2^-$) in ^{11}C. The squares are from Ref. [19], and the filled circle with error bar is suggested by this paper.

[36] and the $9/2^-$ member of the $K^\pi = 3/2^-$ rotational band [19] might be two closely lying states at approximately 12.65 MeV. Unfortunately, they cannot be separated in the present paper. Further experiment is required to clarify such doublet structure.

B. Rotational bands

Regarding rotational bands in ^{11}C, three rotational bands ($K^\pi = 5/2^+, 3/2^+, 3/2^-$) with large inertia momentum were predicted, and some members were observed [16,19]. However, some spin parities of these members have not been reliably determined experimentally. Two bands with even parity have been confirmed [18,19]. The $K^\pi = 5/2^+$ rotational band has 6.905-, 8.655-, 10.679-, and 13.4-MeV members, and the $K^\pi = 3/2^+$ one has 7.4997-, 8.699-, 10.083-, and 12.2-MeV members [16,18,19,31].

However, there are still doubts about the negative-parity rotational band ($K^\pi = 3/2^-$). Among the members of the negative-parity band, the band head is the $3/2^-$ state, which is observed at $E_x = 8.10$ MeV in this paper. The second member in the mirror ^{11}B nucleus was predicted to be the third $5/2^-$ state [12], and hence the corresponding state in the ^{11}C nucleus was thought to be the 9.78-MeV state [19]. However, Wiescher *et al.* [34] recently identified that the 9.38-MeV state has a spin parity of $5/2^-$, and it would preferentially become the third $5/2^-$ state. It should be noted that this state has a branching ratio of α decay of nearly 100%. In addition, the 9.78-MeV candidate state was also doubted by Yamaguchi *et al.* [19] because its branching ratio is not large enough. Therefore, the 9.38-MeV state observed both in this paper and in Ref. [34] is suggested to be the second member, as drawn with a filled circle in Fig. 8. The third member was assigned to be the resonance at 11.03 MeV, while its spin has not been clearly determined [19]. We find that this resonance is much weaker than the 11.44-MeV state, the spin parity of which is also unclear. Therefore, the possible candidate at 11.44 MeV should be studied in further experiments. The fourth member at approximately 12.65 MeV is more promising, which was observed as a strong resonance in previous measurements [16,18,19] and also in the present paper, if its undetermined spin parity and possible state mixing are not problems.

After assigning the second member to the 9.38-MeV state, this rotational band becomes smoother, as shown in Fig. 8. Here, we derived a rotational parameter of $\hbar^2/2I$ of 0.216 MeV, suggesting a large deformation. For comparison, the rotational band based on the Hoyle state has a $\hbar^2/2I$ of 0.300 MeV [37].

V. SUMMARY

We measured the ^{12}C(^{11}C, ^{7}Be + α) reaction with 25-MeV/nucleon ^{11}C bombarding a 50-mg/cm^2 carbon target to study the cluster states in ^{11}C. Excited states above the α-decay threshold up to 14 MeV were populated and their α-decay fragments were detected coincidentally with a DSSD-CsI(Tl) telescope.

The excitation function for the $\alpha + {}^7$Be channel was reconstructed using the invariant-mass method. The 8.10-MeV state was observed as a strong resonance, supporting previous assignment as the head of the $K^\pi = 3/2^-$ rotational band [19] that has a three-center ($2\alpha + {}^3$He) cluster structure. The existence of the 9.38-MeV state was confirmed, and assigned as the second member of the $K^\pi = 3/2^-$ rotational band for the first time, rather than the 9.78-MeV state. This assignment made the band smoother. Compared with the previous results in the region of $E_x = 11.9-13.0$, the 12.2-MeV state was suggested to be the $9/2^+$ member of the $K^\pi = 3/2^+$ rotational band, and the 12.65-MeV state was suggested to be the $9/2^-$ member of the $K^\pi = 3/2^-$ rotational band. We derived a rotational parameter $\hbar^2/2I$ of 0.216 MeV for this rotational band.

A few triplefold coincidence events of $2\alpha + {}^3$He were observed, which possibly indicate a three-center structure of some resonant states in ^{11}C. However, the present low statistics prevent drawing any strong conclusions. Further experiments are needed to study the cluster structure of ^{11}C in detail and to determine the spin parities for some important states.

ACKNOWLEDGMENT

This work has been supported by the National Natural Science Foundation of China (Grants No. 10175091, No. 11305007, and No. 11961141004).

[1] W. Vonoertzen, M. Freer, and Y. Kanada-En'yo, Nuclear clusters and nuclear molecules, Phys. Rep. **432**, 43 (2006).

[2] M. Freer, The clustered nucleus-cluster structures in stable and unstable nuclei, Rep. Prog. Phys. **70**, 2149 (2007).

[3] K. Ikeda, N. Takigawa, and H. Horiuchi, The systematic structure-change into the molecule-like structures in the self-conjugate 4n nuclei, Prog. Theor. Phys. Suppl. **E68**, 464 (1968).

[4] M. Freer, H. Horiuchi, Y. Kanada-En'yo, D. Lee, and U.-G. Meißner, Microscopic clustering in light nuclei, Rev. Mod. Phys. **90**, 035004 (2018).

[5] L. R. Hafstad and E. Teller, The alpha-particle model of the nucleus, Phys. Rev. **54**, 681 (1938).

[6] R. B. Wiringa, S. C. Pieper, J. Carlson, and V. R. Pandharipande, Quantum Monte Carlo calculations of A = 8 nuclei, Phys. Rev. C **62**, 014001 (2000).

[7] A. Tohsaki, H. Horiuchi, P. Schuck, and G. Röpke, Alpha Cluster Condensation in ^{12}C and ^{16}O, Phys. Rev. Lett. **87**, 192501 (2001).

[8] R. Smith, T. Kokalova, C. Wheldon, J. E. Bishop, M. Freer, N. Curtis, and D. J. Parker, New Measurement of the Direct 3α Decay from the ^{12}C Hoyle State, Phys. Rev. Lett. **119**, 132502 (2017).

[9] F. Hoyle, On nuclear reactions occurring in very hot stars. I. The synthesis of elements from carbon to nickel, Astrophys. J. Suppl. Series **1**, 121 (1955).

[10] M. Wiescher, R. N. Boyd, S. L. Blatt, L. J. Rybarcyk, J. A. Spizuoco, R. E. Azuma, E. T. H. Clifford, J. D. King, J. Görres, C. Rolfs, and A. Vlieks, ^{11}C level structure via the ^{10}B(p, γ) reaction, Phys. Rev. C **28**, 1431 (1983).

[11] Y. Kanada-En'yo, Three-center cluster states in ^{11}C and ^{11}B, Mod. Phys. Lett. A **21**, 2403 (2006).

[12] T. Suhara and Y. Kanada-En'yo, Cluster structures in ^{11}B, Phys. Rev. C **85**, 054320 (2012).

[13] T. Yamada and Y. Funaki, Three-body cluster structures and Hoyle-analogue states in ^{11}B, Prog. Theor. Phys. Suppl. **196**, 388 (2012).

[14] T. Kawabata, H. Akimune, H. Fujimura, H. Fujita, Y. Fujita, M. Fujiwara, K. Hara, K. Y. Hara, K. Hatanaka, T. Ishikawa, M. Itoh, J. Kamiya, S. Kishi, M. Nakamura, K. Nakanishi, T. Noro, H. Sakaguchi, Y. Shimbara, H. Takeda, A. Tamii *et al.*, Isovector and isoscalar spin-flip M1 strengths in ^{11}B, Phys. Rev. C **70**, 034318 (2004).

[15] T. Kawabata, H. Akimune, H. Fujita, Y. Fujita, M. Fujiwara, K. Hara, K. Hatanaka, M. Itoh, Y. Kanada-En'yo, S. Kishi, K. Nakanishi, H. Sakaguchi, Y. Shimbara, A. Tamii, S. Terashima, M. Uchida, T. Wakasa, Y. Yasuda, H. P. Yoshida, and M. Yosoi, $2\alpha + t$ cluster structure in ^{11}B, Phys. Lett. B **646**, 6 (2007).

[16] N. Soić, M. Freer, L. Donadille, N. M. Clarke, P. J. Leask, W. N. Catford, K. L. Jones, D. Mahboub, B. R. Fulton, B. J. Greenhalgh, D. L. Watson, and D. C. Weisser, Alpha-decay of excited states in ^{11}C and ^{11}B, Nucl. Phys. A **742**, 271 (2004).

[17] N. Soić, M. Freer, L. Donadille, N. M. Clarke, P. J. Leask, W. N. Catford, K. L. Jones, D. Mahboub, B. R. Fulton, B. J. Greenhalgh, D. L. Watson, and D. C. Weisser, Three-centre cluster structure in ^{11}C and ^{11}B, J. Phys. G: Nucl. Part. Phys. **31**, S1701 (2005).

[18] M. Freer, N. L. Achouri, C. Angulo, N. I. Ashwood, D. W. Bardayan, S. Brown, W. N. Catford, K. A. Chipps, N. Curtis, P. Demaret, C. Harlin, B. Laurent, J. D. Malcolm, M. Milin, T. Munoz-Britton, N. A. Orr, S. D. Pain, D. Price, R. Raabe, N. Soic *et al.*, Resonances in ^{11}C observed in the ^{4}He(^{7}Be, α)^{7}Be and ^{4}He(^{7}Be, p)^{10}B reactions, Phys. Rev. C **85**, 014304 (2012).

[19] H. Yamaguchi, D. Kahl, Y. Wakabayashi, S. Kubono, T. Hashimoto, S. Hayakawa, T. Kawabata, N. Iwasa, T. Teranishi, Y. K. Kwon, D. N. Binh, L. H. Khiem, and N. N. Duy, α-resonance structure in ^{11}C studied via resonant scattering of ^{7}Be + α and with the ^{7}Be(α, p) reaction, Phys. Rev. C **87**, 034303 (2013).

[20] Z. Sun, W. L. Zhan, Z. Y. Guo, G. Xiao, and J. X. Li, RIBLL, the radioactive ion beam line in Lanzhou, Nucl. Instrum. Methods Phys. Res. Sect. A **503**, 496 (2003).

[21] J. J. He, S. W. Xu, P. Ma, J. S. Wang, Y. Y. Yang, J. B. Ma, L. Y. Zhang, L. Li, X. Q. Yu, S. L. Jin, J. Hu, S. Kubono, S. Z. Chen, N. T. Zhang, M. L. Liu, X. G. Lei, Z. Y. Sun, Y. H. Zhang, X. H. Zhou, H. S. Xu *et al.*, A new low-energy radioactive beam line for nuclear astrophysics studies in china, Nucl. Instrum. Methods Phys. Res. Sect. A **680**, 43 (2012).

[22] K.-H. Schmidt, E. Hanelt, H. Geissel, G. Münzenberg, and J. Dufour, The momentum-loss achromat—A new method for the isotopical separation of relativistic heavy ions, Nucl. Instrum. Methods Phys. Res. Sect. A **260**, 287 (1987).

[23] J. X. Li, W. L. Zhan, Z. Y. Guo, Z. Y. Sun, G. Q. Xiao, J. C. Wang, X. W. Meng, S. H. Jiang, L. J. Qin, W. S. Zhang, and Q. J. Wang, TOF measurement in RIBLL, High Ener. Phys. Nucl. Phys. (in Chinese) **23**, 231 (1999).

[24] J. F. Ziegler, M. Ziegler, and J. Biersack, SRIM—The stopping and range of ions in matter (2010), Nucl. Instrum. Methods Phys. Res. Sect. B **268**, 1818 (2010).

[25] Micron Semiconductor Ltd. Silicon detector catalogue, http://www.micronsemiconductor.co.uk/silicon-detector-catalogue/. Accessed 12 August 2019.

[26] O. Tarasov and D. Bazin, LISE++: Radioactive beam production with in-flight separators, Nucl. Instrum. Methods Phys. Res. Sect. B **266**, 4657 (2008).

[27] A. Fomichev, I. David, S. Lukyanov, Y. Penionzhkevich, N. Skobelev, O. Tarasov, A. Matthies, H.-G. Ortlepp, W. Wagner, M. Lewitowicz, M. Saint-Laurent, J. Corre, Z. Dlouhý, I. Pecina, and C. Borcea, The response of a large CsI(Tl) detector to light particles and heavy ions in the intermediate energy range, Nucl. Instrum. Methods Phys. Res. Sect. A **344**, 378 (1994).

[28] Q. Xiang, D. Tian, F. Hao, C. Chu, G. Ding, J. Zeng, and F. Luo, Self-calibration method for cerium-doped lanthanum bromide scintillator detector in the 0.1–2.0 MeV energy range, J. Radioanal. Nucl. Chem. **299**, 1439 (2014).

[29] Z. H. Yang, Y. L. Ye, Z. H. Li, J. L. Lou, J. S. Wang, D. X. Jiang, Y. C. Ge, Q. T. Li, H. Hua, X. Q. Li, F. R. Xu, J. C. Pei, R. Qiao, H. B. You, H. Wang, Z. Y. Tian, K. A. Li, Y. L. Sun, H. N. Liu, J. Chen *et al.*, Helium-helium clustering states in ^{12}Be, Phys. Rev. C **91**, 024304 (2015).

[30] J. Li, Y. L. Ye, Z. H. Li, C. J. Lin, Q. T. Li, Y. C. Ge, J. L. Lou, Z. Y. Tian, W. Jiang, Z. H. Yang, J. Feng, P. J. Li, J. Chen, Q. Liu, H. L. Zang, B. Yang, Y. Zhang, Z. Q. Chen, Y. Liu, X. H. Sun *et al.*, Selective decay from a candidate of the σ-bond linear-chain state in ^{14}C, Phys. Rev. C **95**, 021303(R) (2017).

[31] From ENSDF database as of 19 November 2019. Version available at http://www.nndc.bnl.gov/ensarchivals/.

[32] D. L. Price, M. Freer, N. I. Ashwood, N. M. Clarke, N. Curtis, L. Giot, V. Lima, P. McEwan, B. Novatski, N. A. Orr, S. Sakuta, J. A. Scarpaci, D. Stepanov, and V. Ziman, α decay of excited states in ^{14}C, Phys. Rev. C **75**, 014305 (2007).

[33] M. Assié, J. A. Scarpaci, D. Lacroix, J. C. Angélique, D. Bazin, D. Beaumel, Y. Blumenfeld, W. N. Catford, M. Chabot, A. Chatterjee, M. Fallot, H. Iwasaki, F. Maréchal, D. Mengoni, C. Monrozeau, J. Nyberg, C. Petrache, F. Skaza, and T. Tuna,

Neutron correlations in ^{6}He viewed through nuclear break-up, Eur. Phys. J. A **42**, 441 (2009).

[34] M. Wiescher, R. J. deBoer, J. Gorres, and R. E. Azuma, Low energy measurements of the ^{10}B$(p,\alpha)^{7}$Be reaction, Phys. Rev. C **95**, 044617 (2017).

[35] I. Lombardo, D. Dell'Aquila, F. Conte, L. Francalanza, M. La Cognata, L. Lamia, R. La Torre, G. Spadaccini, C. Spitaleri, and M. Vigilante, New investigations of the ^{10}B$(p,\alpha_0)^{7}$Be reaction at bombarding energies between 0.6 and 1MeV, J. Phys. G: Nucl. Part. Phys. **43**, 045109 (2016).

[36] J. Jenkin, L. Earwaker, and E. Titterton, The ^{10}B$(p,\alpha)^{7}$Be reaction between 2 and 11 MeV, Nucl. Phys. **50**, 516 (1964).

[37] A. Ogloblin, A. Demyanova, A. Danilov, S. Dmitriev, T. Belyaeva, S. Goncharov, V. Maslov, Y. Sobolev, W. Trzaska, and S. Khlebnikov, Rotational band in ^{12}C based on the Hoyle state, EPJ Web Conf. **66**, 02074 (2014).